Precision Enhancement of an Aerosols Optical Characterization Device

M. J. Rodríguez Guzmán*, E. Montilla Rosero , and D. Bolaños Marín

School of Sciences Applied and Engineering, Universidad EAFIT, Medellín, Colombia
**Corresponding author: mjrodrigu1@eafit.edu.co*

Compiled June 1, 2022

Reassembly and improvement of an aerosols chamber is presented here, looking for precision enhancement through optomechanical modifications and subsystems redesign. To test the efficiency, it was experimentally obtained the volumetric and particle LDR of calcium carbonate ($CaCO_3$), resulting in average values of 0.55 and 0.75 respectively, with percentage errors less than 5% according to theoretically measurements derived from simulations developed by [1]. Finally, some considerations that should be taken into account for future works are presented.

Keywords: ***atmospheric aerosols, calibration factor, depolarization, LDR.***

1. INTRODUCTION

Medellín air quality is constantly disturbed by atmospheric aerosols (particles suspended in the atmosphere [2]) which causes repeated and worrying environmental crisis in the city [3]. In order to solve this problem, it is first needed to identify the pollutants sources, by analyzing their physical and chemical characteristics, e.g. the particle surface-area, volume and mass concentration, mean particle size and the volume extinction coefficient [4], so afterwards strategies can be planned to mitigate their impact. These kind of parameters can only be known with high temporal and spatial resolution, using LIDAR instruments, like in the NASA and CNES project, CALIPSO, where influence of clouds and aerosols in air quality was studied, employing a depolarization LIDAR [5].

Otherwise, aerosols impact on the atmosphere have been studied in laboratory chambers, as well. For example, the research done by Sakai et al. to analyze the linear polarization ratio (δ_p) of three kinds of particles was implemented in a laboratory pipe, composed of a clean air pump, an aerosol generator, a jet impactor, an optical particle counter (OPC) and a polarization LIDAR [6]. Another interesting work was done by Järvinen et al. in which it was studied the optical properties of dust aerosols with an *in situ* scattering and depolarization instrument, located at a cloud simulation chamber of 84 m^3, where a thermal housing controlled the temperature and relative humidity (RH) [7].

Later on, Massabò et al. constructed a 2.2 m^3 chamber to analyze the interaction of bacteria viability with air quality, in which temperature and RH control were included [8]. Afterward, Kaltsonoudis et al. studied the evolution of atmospheric particulate matter, following their chemical and physical processes in the air. It was achieved through a portable dual-smog-chamber of 1.5 m^3 each, surrounded by UV lamps and with temperature and RH sensors inside [9].

Based on all of these works, from 2017 to 2020, the Atmospheric Optics branch from the Applied Optics investigation group from EAFIT University designed and built an atmospheric chamber [1, 10, 11], where the optical and physical properties of some aerosols were studied, as well as the influence of meteorological variables on them. The system was composed by a 0.015 m^3 chamber, an aerosols fluidizer, an optical system to send and receive the backscattered light and a temperature and RH control.

Although the complete device was dismantled once the objectives were achieved, recently emerged the necessity to reassembly it and carry out some technical changes which induce a value's accuracy improvement and a simple user operation, since this project can contribute to characterize several types of aerosols, in order to have reference data for LIDAR measurements and

later studies in the Atmospheric Optics branch.

2. METHODOLOGY

A. Depolarization and LDR

Understanding the physical concepts and evaluating the way they can be measured was the initial step to reach the final goal. The first concept is *depolarization*, the capacity of a medium to modify the polarization initial state. Then, this alteration can be measured by the LDR and, more specifically, with the Stokes parameters that give information about the light-medium interaction with the Müller matrix, in the following way:

$$(I, Q, U, V) = \boldsymbol{F} \cdot (I_0, Q_0, U_0, V_0) \tag{1}$$

Being the variables with subscripts the initial Stokes parameters from the incident light and $\boldsymbol{F}$ the medium matrix, described like:

$$\begin{bmatrix} I \\ Q \\ U \\ V \end{bmatrix} = \begin{bmatrix} f_{11} & f_{12} & f_{13} & f_{14} \\ f_{21} & f_{22} & f_{23} & f_{24} \\ f_{31} & f_{32} & f_{33} & f_{34} \\ f_{41} & f_{42} & f_{43} & f_{44} \end{bmatrix} \begin{bmatrix} I_0 \\ Q_0 \\ U_0 \\ V_0 \end{bmatrix} \tag{2}$$

Nevertheless, the most practical notation to estimate the polarimetric properties within a scatter medium, like the atmosphere, is the Perrin notation, in which the Müller matrix is described in terms of the orientation angle of the particle, θ. Thus, assuming a symmetry plane in the scattering particles and aleatory orientation, $\boldsymbol{F}$ can be written as:

$$\boldsymbol{F} = \begin{bmatrix} a_1(\theta) & b_1(\theta) & 0 & 0 \\ b_1(\theta) & a_2(\theta) & 0 & 0 \\ 0 & 0 & a_3(\theta) & b_2(\theta) \\ 0 & 0 & -b_2(\theta) & a_4(\theta) \end{bmatrix} \tag{3}$$

With this information, now the *linear depolarization ratio* (LDR or δ) can be defined as follow:

$$\delta = \frac{a_1(180^\circ) - a_2(180^\circ)}{a_1(180^\circ) + a_2(180^\circ)} \tag{4}$$

where a_1 represents the I polarization and a_2 represents the Q one (by comparing equation 3 with equation 2).

In this order of ideas, δ gives information about the contribution of vertical and horizontal oscillations of the electrical field after being scattered.

Experimentally, this parameter is measured as the ratio between the perpendicular and the parallel intensities, detected through a PBS and two PMT, scaled by a calibration factor, which tends to correct the PBS crosstalk and reduce optical instruments error. In this work, Delta90 calibration method was implemented, using 0° and 90°, due to the system characteristics.

$$\eta^* = \frac{I_\perp}{I_\parallel}(0^\circ, 90^\circ)\,;\, \eta^*_{\Delta 90} = \sqrt{(\eta^*(0^\circ + \varepsilon)\eta^*(90^\circ + \varepsilon))} \tag{5}$$

$$\eta_{\Delta 90} = \frac{1}{K}\eta^*_{\Delta 90} \tag{6}$$

where ε represents the PBS rotation error (which is 0 in this case) and K is a calibration factor correction, which will be consider ideal ($K = 1$), since optical elements where characterized in a previous work [1] and it was not found any representative depolarizing effect.

Then the incoming steps are followed:

1. Calculate apparent volume linear depolarization ratio (VLDR)
$$\delta^* = \frac{1}{\eta_{\Delta 90}} \frac{I_\perp(0^\circ)}{I_\parallel 0^\circ} \tag{7}$$
2. Introduce polarization cross-talk correction parameters to calculate VLDR
$$\delta_v = \frac{\delta^* (G_T + H_T) - (G_R + H_R)}{(G_R - H_R) - \delta^* (G_T - H_T)} \tag{8}$$
where $G_{T,R}$ and $H_{T,R}$ correct systematic error.
3. Calculate particle LDR (PLDR)
$$\delta_p = \frac{(1 + \delta_m)\,\delta_v R - (1 + \delta_v)\,\delta_m}{(1 + \delta_m)\,R - (1 + \delta_v)} \tag{9}$$
knowing that δ_m is molecules LDR (taken from literature [12]) and R is the backscatter ratio, calculated in [1].

B. Optomechanical improvements

An important statement during this project was reducing the chamber leakages, in order to preserve the flow inside. Therefore, the laser beam entrance and exit pieces were redesigned based on a sandwich model with o-rings in between and a cleaning system was created by making a square hole in the frontal wall, in order to build a sealed door with a rubber edge and a nylon plug, with an o-ring inside as well.

In the interest of proving the system was leaks-free a vacuum test was accomplished with the new pieces, while the relative humidity percentage (%RH) was measured. As expected, this variable decreased 20% in about 10 min (see figure 1), revealing a great seal on the chamber

C. Fluidizer system

The fluidizer system was redesigned in two crucial parts: the aerosols feeder and the particles carriage. The first one consist of a cylinder with a funnel inside, which the smaller diameter is 1/8" to allow a controlled passage of the particles (see figure 2), meanwhile the last one led to the use of a wire reinforced hose, which has a great resistance and enables the correct flow stream.

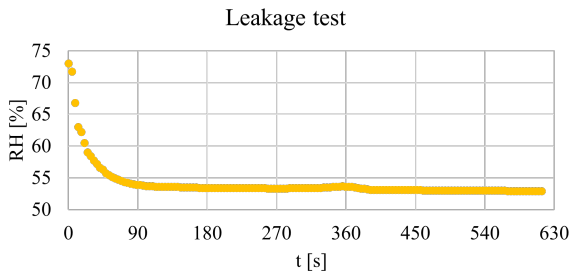

Fig. 1. Chamber leakages test.

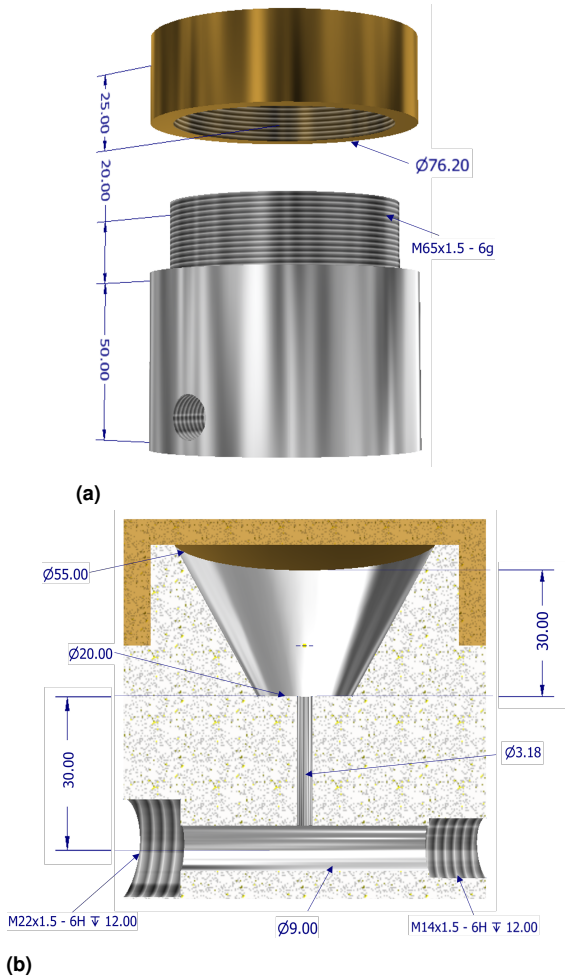

Fig. 2. Aerosols feeder design (a) and transversal view (b).

Additionally, the optical particle counter (OPC) was replaced in this project, due to the previously used sensor was out of stock at the moment of testing. Thus, the whole fludizer system (feeder, carriage and OPC) needed a characterization to get to know the ideal working flow to obtain the greater number of PM2.5 inside the chamber. Figure 3 shows the two flows that had the best behaviour, being the 12 L/min the best of all, reason why it was chosen. It is also exposed an unwanted characteristic of the OPC and it was its saturation measurement, as the maximum possible value was 1000 $\mu g/m^3$ and, in the conditions that it was put through, that number was exceeded for higher flows than 15 L/min and under high humidity levels, as it will be seen in next sections.

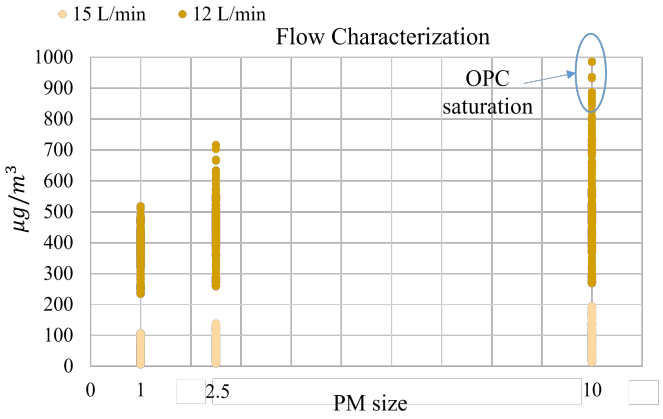

Fig. 3. Fluidizer flow characterization.

D. User operation

The software to obtain and process data is MATLAB, divided in three codes: the first one transfers the signals information from the oscilloscope to the folder selected in the PC, the second one imports the data saved from the oscilloscope, filters it, subtracts ambient noise (if needed) and plots and saves the resulting data.Finally, in the third code, the calibration signals are loaded and the calibration factor is computed, so the VLDR and PLDR of the aerosols selected is determined and plotted. Consult the User Manual for complete information about the system operation.

3. RESULTS AND DISCUSSION

There were carried out several tests, expecting to get a similar behaviour obtained before by the Applied Optics investigation group from EAFIT University. Nevertheless, the system characteristics varied greatly, implying a new state of art review and reevaluate some theoretical concepts to get good results. For example, in the previous work the calibration method was done with $\pm 45°$, as it is suggested in [13], but for this project it was noticed that the reflected signal is much smaller than the transmitted one, which means that the changes inside the chamber will be seen especially in the first one. Thus, it was more convenient performing the calibration with $0°$ and $90°$, resulting in the mean value exhibited in figure 4, which was obtained using equations 5 and 6 with $\varepsilon = 0$ and $K = 1$.

As it is revealed, the calibration factor does not have the ideal value ($\eta_{\Delta 90} = 1$) that was anticipated. The reasons for that lie mainly in systematic errors, such as "rotational misalignment [of the optical elements] and non-ideal laser polarisation" [13], or in an unexpected depolarization created by a chamber's component. However, this number should not affect the VLDR and PLDR calculus, since it must correct the base errors that the system possess.

Once this parameter was computed, the VLDR was estimated, using equations 7 and 8, where $G_{R,T}$ and $H_{R,T}$ were assumed as ideal ($G_{R,T} = H_T = 1$; $H_R = -1$), ac-

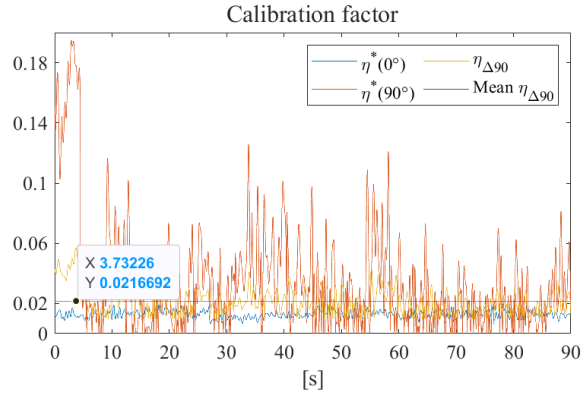

Fig. 4. Calibration factor $\eta_{\Delta 90}$.

cording to [1]. From all the tests done, there were two remarkable that can be seen in figures 5 and 6, the former represents standard laboratory temperature (∼25°C) and %RH (∼43%) and the latter is for the highest %RH (75-100%) and temperature of 26.5°C). In both situations, the VLDR measurements are consistent, and close to the values achieved in a previous work (see table 1, where values reported in [1] were taken as theoretical to estimate the percentage error and the experimental values are result of the average of multiples tests).

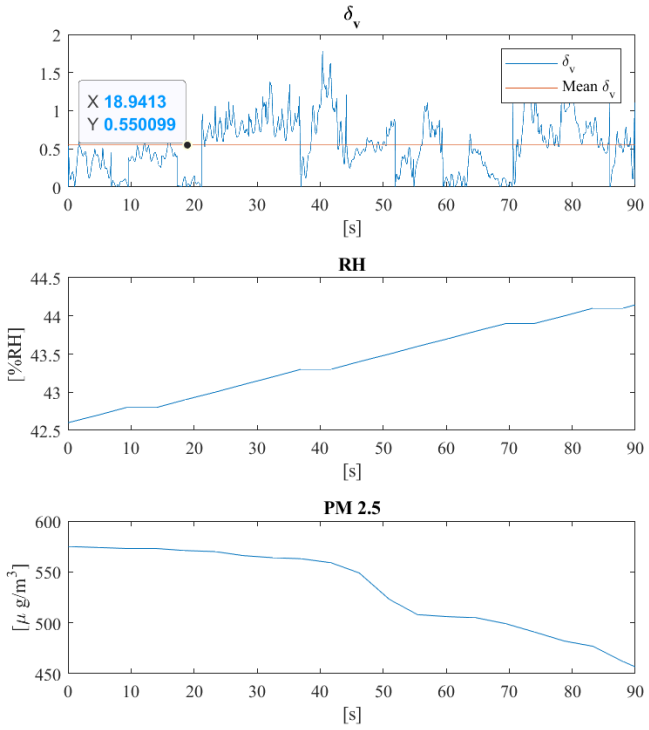

Fig. 5. Measurements obtained under standard laboratory conditions.

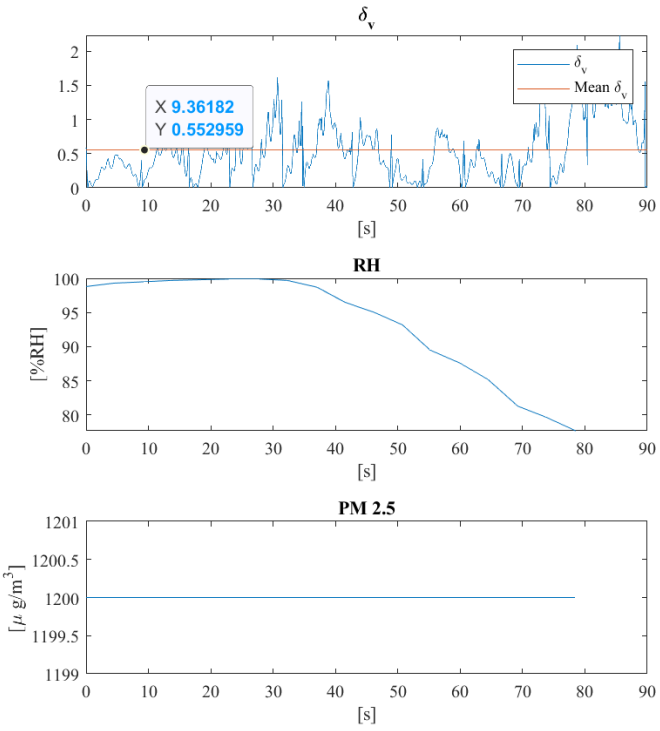

Fig. 6. Measurements taken under high %RH values.

	δ_v		δ_p	
	Experimental	**Simulation**	**Experimental**	**Simulation**
Previous work [1]	0.6	0.53	0.8	0.72
Current work	0.55	-	0.75	-
% Error	8.33%	3.77%	6.25%	4.17%

Table 1. Previous and current work comparison.

4. CONCLUSIONS AND FUTURE WORKS

Bearing in mind all the information exposed in this document, it can be stated that the recovery of the optical characterization device was successful, and it was adapted for the management of any user, since it is left as a functional system and the User Manual facilitate its operation. Additionally, it was seen that the optomechanical improvements developed introduced intrinsic changes to the chamber that affected some parameters and redefined them to this specific case, which led to identify an essential requirement: to analyze the calibration procedure for each system, since the conditions and the signals received can vary from one to another and the $\eta_{\Delta 90}$ ratio must be chosen in the most convenient way to correct the PBS crosstalk.

Besides, considering future works it is highly recommended taking into account include a filter right before the clean air entrance, since the compressor add a measurement error during its charge, due to the dust present in the room. Furthermore, it is priority changing the OPC, due to the actual one reaches its limit value easily under

the continuous work conditions of the system. Finally, it is highly suggested including more flow meter, specifically right before the aerosol's feeder, to have a better control on the input variables of the chamber.

ACKNOWLEDGMENTS

The authors thank to the Applied Optics investigation group from EAFIT University, the technical support staff (physics laboratories, metalworking, design and mechatronics workshops) and family and friends for emotional support.

REFERENCES

1. D. Bolaños Marín, "HERRAMIENTA DE LABORATORIO PARA LA CARACTERIZACIÓN ÓPTICA DE AEROSOLES ATMOSFÉRICOS," (2020).
2. B. Allen, "Atmospheric Aerosols: What Are They, and Why Are They So Important?" (2015).
3. Alcaldía de Medellín, "Decreto 0096 de 2021," (2021).
4. C. Weitkamp, *Lidar: Range-Resolves Optical Remote Sensing of the Atmosphere* (Springer, Geesthacht, 2005).
5. K. Lorentz, "NASA - CALIPSO Spacecraft and Instruments," (2006).
6. T. Sakai, T. Nagai, Y. Zaizen, and Y. Mano, "Backscattering linear depolarization ratio measurements of mineral, sea-salt, and ammonium sulfate particles simulated in a laboratory chamber," Appl. Opt. **49**, 4441–4449 (2010).
7. E. Järvinen, O. Kemppinen, T. Nousiainen, T. Kociok, O. Möhler, T. Leisner, and M. Schnaiter, "Laboratory investigations of mineral dust near-backscattering depolarization ratios," J. Quant. Spectrosc. Radiat. Transf. **178**, 192–208 (2016).
8. D. Massabò, S. Giulia Danelli, P. Brotto, A. Comite, C. Costa, A. Di Cesare, J. François Doussin, F. Ferraro, P. Formenti, E. Gatta, L. Negretti, M. Oliva, F. Parodi, L. Vezzulli, and P. Prati, "ChAMBRe: A new atmospheric simulation chamber for aerosol modelling and bio-aerosol research," Atmospheric Meas. Tech. **11**, 5885–5900 (2018).
9. C. Kaltsonoudis, S. D. Jorga, E. Louvaris, K. Florou, and S. N. Pandis, "A portable dual-smog-chamber system for atmospheric aerosol field studies," Atmospheric Meas. Tech. **12**, 2733–2743 (2019).
10. M. Hoyos Restrepo and E. Montilla Rosero, "Diseño e implementación de un control de temperatura aplicado a una cámara de aerosoles atmosféricos," pp. 1–7 (2015).
11. M. Hoyos Restrepo and E. Montilla Rosero, "Design of an urban atmospheric aerosols chamber for laboratory studies," pp. 1–6 (2018).
12. A. Behrendt and T. Nakamura, "Calculation of the calibration constant of polarization lidar and its dependency on atmospheric temperature," Opt. Express **10**, 805 (2002).
13. V. Freudenthaler, "About the effects of polarising optics on lidar signals and the Δ90 calibration," Tech. rep., Ludwig-Maximilians-Universität, Munich (2016).